Diabetologia (2010) 53:2629–2640
DOI 10.1007/s00125-010-1894-6

ARTICLE

Deficiency of CB2 cannabinoid receptor in mice improves insulin sensitivity but increases food intake and obesity with age

J. Agudo · M. Martin · C. Roca · M. Molas · A. S. Bura · A. Zimmer · F. Bosch · R. Maldonado

Received: 16 February 2010 / Accepted: 24 June 2010 / Published online: 11 September 2010

Abstract
Aims/hypothesis The endocannabinoid system has a key role in energy storage and metabolic disorders. The endocannabinoid receptor 2 (CB2R), which was first detected in immune cells, is present in the main peripheral organs responsible for metabolic control. During obesity, CB2R is involved in the development of adipose tissue inflammation and fatty liver. We examined the long-term effects of CB2R deficiency in glucose metabolism.
Methods Mice deficient in CB2R ($Cb2^{-/-}$ [also known as *Cnr2*]) were studied at different ages (2–12 months). Two-month-old $Cb2^{-/-}$ and wild-type mice were treated with a selective CB2R antagonist or fed a high-fat diet.
Results The lack of CB2R in $Cb2^{-/-}$ mice led to greater increases in food intake and body weight with age than in $Cb2^{+/+}$ mice. However, 12-month-old obese $Cb2^{-/-}$ mice did not develop insulin resistance and showed enhanced insulin-stimulated glucose uptake in skeletal muscle. In agreement, adipose tissue hypertrophy was not associated with inflammation. Similarly, treatment of wild-type mice with CB2R antagonist resulted in improved insulin sensitivity. Moreover, when 2-month-old $Cb2^{-/-}$ mice were fed a high-fat diet, reduced body weight gain and normal insulin sensitivity were observed.
Conclusions/interpretation These results indicate that the lack of CB2R-mediated responses protected mice from both age-related and diet-induced insulin resistance, suggesting that these receptors may be a potential therapeutic target in obesity and insulin resistance.

Keywords Endocannabinoids · Food intake · Glucose uptake · Insulin resistance · Obesity

Abbreviations

AKT	Protein kinase B
BAT	Brown adipose tissue
CB1R	Endocannabinoid receptor 1
CB2R	Endocannabinoid receptor 2
FDG	2-[^{18}F]Fluoro-2-deoxy-D-glucose
GSK3B	Glycogen synthase kinase 3 beta
HFD	High-fat diet

J. Agudo and M. Martin contributed equally to this work.

Electronic supplementary material The online version of this article (doi:10.1007/s00125-010-1894-6) contains supplementary material, which is available to authorised users.

J. Agudo · C. Roca · M. Molas · F. Bosch
Center of Animal Biotechnology and Gene Therapy, Department of Biochemistry and Molecular Biology, School of Veterinary Medicine, Universitat Autònoma de Barcelona, Bellaterra, Spain

J. Agudo · C. Roca · M. Molas · F. Bosch
Centro de Investigación Biomédica en Red de Diabetes y Enfermedades Metabólicas Asociadas (CIBERDEM)
URL: www.ciberdem.org

M. Martin · A. S. Bura · R. Maldonado (✉)
Laboratori de Neurofarmacologia, Facultat de Ciències de la Salut i de la Vida, Universitat Pompeu Fabra,
C/Dr Aiguader 88,
08003 Barcelona, Spain
e-mail: rafael.maldonado@upf.edu

A. Zimmer
Institute of Molecular Psychiatry, University of Bonn,
Bonn, Germany

F. Bosch (✉)
Center of Animal Biotechnology and Gene Therapy,
Edifici H, Universitat Autònoma de Barcelona,
Bellaterra 08193, Spain
e-mail: Fatima.Bosch@uab.es

IR	Insulin receptor
IRS1	Insulin receptor substrate 1
LPS	Lipopolysaccharide
MAPK	Mitogen-activated protein kinase
WAT	White adipose tissue

Introduction

The endocannabinoid system plays an important role in the control of food intake and metabolism and participates in the pathophysiology of obesity and type 2 diabetes [1, 2]. Two different endocannabinoid receptors, CB1R and CB2R [3, 4], have been identified. Peripheral CB1R is located in adipocytes, hepatocytes, skeletal muscle and pancreas [1, 5]. Overactivation of the endocannabinoid system has been reported in rodent models of obesity [1, 6, 7] and in obese and type 2 diabetic patients [8]. Moreover, overactivity of the endocannabinoid system in obese patients has been associated with enhanced visceral rather than subcutaneous fat mass [8–10]. These findings suggest that increased activity of the endocannabinoid system in visceral fat may be a key component in the development of insulin resistance. Furthermore, overactivation of CB1R in skeletal muscle promotes insulin resistance [11]; in this regard, pharmacological activation of CB1R activity diminishes mitogen-activated (MAP) kinase- and protein kinase B (PKB)-directed signalling [12]. In the liver, overactivation of CB1R enhances hepatic insulin resistance and lipogenesis [7], while the selective disruption of CB1R in hepatocytes protects mice fed a high-fat diet from liver steatosis and insulin resistance [13]. Moreover, CB1R hyperactivity in adipocytes facilitates fat accumulation and insulin resistance [14]. In cultured pancreatic islets exposure to endocannabinoids increases insulin release [15], suggesting that overactivity of the endocannabinoid system may contribute to the hyperinsulinaemia associated with insulin resistance.

CB2R is mainly located in the cells of the immune system and participates in the modulation of immune responses [16, 17]. In both mice and humans, CB2R is also present in the main peripheral organs responsible for the control of metabolism, including the liver [18], adipose tissue [5, 19–21], skeletal muscle [22] and pancreatic islets [23]. Obesity leads to increased expression of the cannabinoid receptor 2 gene (*Cb2* [also known as *Cnr2*]) both in adipose tissue and liver in high fat fed and *ob*/*ob* mice [24]. However, this expression is predominantly located in the stromal vascular fraction of adipose tissue, while in liver CB2R is present only in the non-parenchymal cell fraction. CB2R deficiency decreases body weight gain during the feeding of a high-fat diet and prevents obesity-associated inflammation, insulin resistance and fatty liver [24]. Nevertheless, the role of long-term CB2R deficiency in the control of whole body metabolism has not been clarified. Here we used *Cb2* knockout mice ($Cb2^{-/-}$) [25] to further evaluate the contribution of CB2R to the regulation of glucose metabolism in young and old mice.

Methods

Animals Male knockout mice deficient in CB2R ($Cb2^{-/-}$) and wild-type littermates ($Cb2^{+/+}$) [25] on a C57Bl/6J background of different ages (2, 6 and 12 months) and maintained under a 12 h light–dark cycle (lights on at 08:00 hours) were used. Mice were fed ad libitum with a standard diet (Basal Purified Diet with 12% energy from fat; Test Diet, Richmond, IN, USA) or, when stated, a high-fat diet (Basal Purified Diet with 60% energy from fat; Test Diet). An additional group of C57Bl/6J wild-type mice were treated with the CB2R inverse agonist SR 144528 (Sanofi Recherche, Montpellier, France; for more information, see Electronic supplementary methods [ESM]). These mice received once daily i.p. injections, on consecutive days, for 28 days of either vehicle (1.8% DMSO, 0.0004% Tween 80 in distilled water) or vehicle plus antagonist (3 mg/kg body weight). Where stated, mice were fasted for 16 h. Body temperature was assessed anally with a thermometer in the morning either at room temperature or at 4°C (cold exposure). Animal procedures were conducted in accordance with the guidelines of the European Communities Directive 86/609/EEC regulating animal research and were approved by the local ethics committee.

Hormone and metabolite determination Serum insulin and leptin were evaluated with ELISA kits (Crystal Chem, Chicago, IL, USA). Serum adiponectin levels were evaluated by radioimmunoassay (Linco Research, St Charles, MO, USA). Non-sterified fatty acids (NEFA) were measured by enzymatic colorimetric assay (NEFA C; Wako Chemicals, Neuss, Germany).

Food intake and leptin-induced anorexigenic effects Mice were housed two per cage. Baseline food intake was measured for 4 weeks. Mice were habituated to the injection procedure (saline, i.p.) for 4 days. Leptin (Prepotech, London, UK) was administered twice a day at a dose of 0.5 μg/g for each injection (i.p.). The decrease in food intake was expressed as a percentage with respect to the baseline and as grams per mouse per day.

Lipopolysaccharide treatment To study the inflammatory response after the acute administration of an external

antigen, mice received an acute i.p. injection of lipopolysaccharide (LPS; 0.5 mg/kg in saline). Blood samples were obtained 3 and 12 h after treatment and TNF-α (3 h after injection) and IL-6 (12 h after injection) concentrations were measured by ELISA (Assay Designs, Ann Arbor, MI, USA).

Insulin and glucose tolerance tests To test insulin tolerance, insulin was administered i.p. (0.75 U/kg; Humilin Regular; Eli Lilly, Indianapolis, IN, USA) to fed mice and tail blood was sampled 0, 15, 30, 45, 60 and 75 min later. For the glucose tolerance test, mice were food-deprived overnight (16 h) and then glucose (1 g/kg i.p.) was administered. Blood glucose was measured from the tail vein 0, 15, 30, 60, 90 and 120 min after glucose injection. Blood glucose was measured with a Glucometer Elite (Bayer Diagnostics, Tarrytown, NY, USA).

Insulin secretion from isolated islets Pancreatic islets were isolated from $Cb2^{+/+}$ and $Cb2^{-/-}$ mice by intraductal injection of collagenase P (1 mg/ml; Roche Molecular Chemicals, Mannheim, Germany) in Hank' balanced salt solution (HBSS) for 10 min at 37°C. Digestion was stopped by washing three times with cold HBSS. Islets were picked by hand. Insulin secretion was measured during a 1 h incubation of islets at 37°C in 1 ml HBSS/0.5% BSA in the presence of 2.8 or 15 mmol/l glucose. After this time, insulin levels in media and insulin content in islets (after homogenisation in ethanol/HCl [10%] solution) were determined with an RIA kit (Linco Research, St Charles, MO, USA).

Gene expression analysis Total RNA was obtained from skeletal muscle, white and brown adipose tissue and liver samples. To synthesise cDNA, 1 μg RNA was used (Omniscript kit; Qiagen, Hilden, Germany). Random primers (Invitrogen, Carlsbad, CA, USA) were used for the reaction in the presence of Protector RNase Inhibitor (Roche Molecular Biochemicals, Mannheim, Germany). RT-PCR was performed in a SmartCycler II (Cepheid, Maurens-Scopont, France) using the QuantiTect SYBR Green PCR Kit (Qiagen). Data were normalised to ribosomal protein S26 (RBS) gene values. Primer sequences are shown in ESM Table 1.

Immunohistochemical and morphometric analysis White and brown adipose tissue, liver and pancreas were fixed for 24 h in formalin, embedded in paraffin and sectioned. To determine white and brown adipose tissue and liver morphology, sections were stained with haematoxylin/eosin. For detection of macrophages, white adipose tissue sections were incubated either with a rabbit anti-F4/80 antibody (Acris, Hidenhausen, Germany) or with a rabbit anti-macrophage galactose-specific lectin-2 (MAC-2) antibody (Cedarlane Laboratories, Burlington, ONT, Canada). For detection of insulin, pancreatic sections were incubated with a guinea pig anti-insulin antibody (Sigma, St Louis, MO, USA). Secondary antibodies were: peroxidase-conjugated goat anti-guinea pig (Dako, Glostrup, Denmark); biotinylated goat anti-rabbit (Pierce Biotechnology, Rockford, IL, USA); horseradish peroxidase-conjugated streptavidin (Molecular Probes, Leiden, the Netherlands). Morphometric analysis is described in the ESM.

PET imaging 2-[^{18}F]Fluoro-2-deoxy-D-glucose (FDG) was used as a radiotracer and was synthesised by Barnatron (Barcelona, Spain) in accordance with the standard procedure [26]. Imaging was performed using a small animal PET scanner (rPET; Suinsa Medical Systems, Madrid, Spain). The methods used for the PET experiment are described in the ESM.

CB2R antagonist treatment in 3T3-L1 adipocytes and Oil Red O staining Maintenance and differentiation of 3T3-L1 cells are described in the ESM. For treatment with the CB2R antagonist (SR 144528), stock solutions of drugs were prepared in DMSO at 10 mmol/l and stored at −20°C. The concentration of solvent in an assay never exceeded 0.1% (vol./vol.). This final concentration was without effect on assays. Cells were cultured in the presence of a final concentration of 100 nmol/l of SR 144528 or the same volume of DMSO. For Oil Red O staining, after being washed twice with PBS buffer, cells were fixed with 10% formaldehyde for 10 min. After two washes in PBS, cells were stained for 20 min with Oil Red O solution (0.18% in 60% isopropanol). Oil Red O was then removed and the cells were washed twice with PBS.

Hepatic and 3T3L1 cell triacylglycerol content The triacylglycerol content of liver and 3T3L1 cells was determined by extracting total lipids from liver samples or cultured cells with chloroform–methanol (2:1 vol./vol.) as described in [27]. Triacylglycerols were quantified spectrophotometrically in the supernatant fractions using an enzymatic assay kit (GPO-PAP; Roche Diagnostics, Basel, Switzerland).

Western blot analysis Tibialis muscles were homogenised in protein lysis buffer. Proteins (50 μg) were separated by 10% SDS-PAGE, transferred to nitrocellulose membranes and probed with primary antibodies against insulin receptor (IR), insulin receptor substrate 1 (IRS1), phosphorylated-Tyr, phospho^{Ser473}-protein kinase B (phospho^{Ser473}-AKT), AKT, phospho^{Ser9}-GSK3B and GSK3 (Cell Signaling Technology, Danvers, MA, USA) and GLUT4 (Chemicon, Billerica, MA, USA) overnight at 4°C. Detection was

performed using horseradish peroxidase-labelled anti-goat IgG or horseradish peroxidase-labelled anti-rabbit IgG (Dako) and ECL Plus Western Blotting Detection Reagent (Amersham, Arlington Heights, IL, USA).

Statistical analysis All values are expressed as mean ± SEM. Differences between groups were compared by Student's *t* test. A p value <0.05 was considered statistically significant.

Results

$Cb2^{-/-}$ mice showed increased food intake, adipose tissue hypertrophy and obesity with age To further determine the role of CB2R in regulating glucose metabolism and energy balance, $Cb2^{-/-}$ mice were examined at different ages. Two-month-old $Cb2^{-/-}$ male mice were normoglycaemic and showed body weight similar to that of age-matched wild-type ($Cb2^{+/+}$) mice (Fig. 1a and ESM Fig. 1a). However, at 6 months of age $Cb2^{-/-}$ mice presented a modest but statistically significant greater body weight (about 6%) compared with wild-type mice, but with normal serum glucose, insulin and leptin levels (Fig. 1a and ESM Fig. 1b, c). These mice also showed a normal beta cell mass (ESM Fig. 1d, e). Moreover, a similar glucose-stimulated insulin release was revealed in islets isolated from $Cb2^{-/-}$ and wild-type mice (ESM Fig. 1f). Twelve-month-old $Cb2^{-/-}$ mice showed 25% greater body weight than wild-type mice (Fig. 1a). This increase was parallel to a two-fold increase in epididymal white adipose tissue (WAT) and interscapular brown adipose tissue (BAT) mass (Fig. 1b). Histological analysis of fat tissue from $Cb2^{-/-}$ mice showed larger white adipocytes than those from wild-type mice (Fig. 1c). Moreover, in $Cb2^{-/-}$ mice lipid droplets in brown adipocytes were larger than those in wild-type mice and, in some adipocytes, lipid deposition appeared unilocular (Fig. 1c). However, the expression of uncoupling protein 1 (*Ucp1)* and peroxisome proliferator-activated receptor gamma coactivator 1-alpha *(Pgc1a)* was not decreased (Fig. 1d) and that of adiponectin (*Adipoq*) was not increased (data not shown) in BAT from $Cb2^{-/-}$ mice. These findings are not consistent with a switch of phenotype from a BAT- to a WAT-like phenotype in $Cb2^{-/-}$ mice. Furthermore, *Pgc1a*, uncoupling protein 2 and 3 (*Ucp2* and *Ucp3)* mRNA levels were normal in skeletal muscle (ESM Fig. 2a) and body temperature was not decreased either at room temperature or after 4 h of cold exposure (ESM Fig. 2b, c). These results suggest that adipose tissue fat accumulation in $Cb2^{-/-}$ mice did not result from decreased thermogenesis and/or energy expenditure. The increase in WAT mass of 12-month-old $Cb2^{-/-}$ mice was consistent with 65% higher circulating leptin levels than in age-matched wild-type mice (Fig. 1e). These $Cb2^{-/-}$ mice showed a 40% increase in food intake (Fig. 1f). Moreover, 1 day after i.p. injection of leptin, $Cb2^{-/-}$ mice displayed a smaller reduction in food intake than wild-type mice (Fig. 1f, g). These results indicate that the mice gradually developed obesity and hypertrophy of adipose tissue with age in association with increased food intake. CB1R activity in the hypothalamus has been related to the enhancement of food intake [6]. However, the expression of cannabinoid receptor 1 (*Cnr1*) was not modified in the cerebellum and hypothalamus of $Cb2^{-/-}$ mice (Fig. 1h). Therefore, the enhanced food intake of $Cb2^{-/-}$ mice was not due to compensatory changes in CB1R receptors in the brain areas regulating feeding behaviour. Parallel to increased fat mass, 12-month-old $Cb2^{-/-}$ mice also showed an increase in the WAT expression of *Cnr1* (Fig. 1h). Similarly, young mice also showed a moderate increase in *Cnr1* expression (ESM Fig. 2d). Nevertheless, no difference in the expression of transient receptor potential vanilloid type 1 (*Trpv1*), which can also be activated by the endocannabinoid anandamide and can regulate lipogenesis [28], was revealed in adipose tissue of $Cb2^{-/-}$ mice at 6 months of age (ESM Fig. 2e). Overactivity of CB1R has also been observed in the adipose tissue of obese rodents [14]. Our findings suggest that fat accumulation in WAT, at least in part due to enhanced food intake, probably contributed to increased *Cnr1* expression in WAT. Consistent with the enhanced fat storage, old

Fig. 1 Enhanced body weight, food intake and hypertrophy of adipose tissue. **a** Body weight of 2-, 6- and 12-month-old $Cb2^{+/+}$ and $Cb2^{-/-}$ mice. **b** Epididymal white adipose tissue (eWAT) and interscapular brown adipose tissue (iBAT) mass in $Cb2^{+/+}$ and $Cb2^{-/-}$ mice. **c** Histological analysis of adipose tissue of $Cb2^{-/-}$ mice, showing cell hypertrophy in WAT and increased lipid droplet size in BAT (×100). **d** *Ucp1* and *Pgc1a* expression in BAT from 12-month-old $Cb2^{-/-}$ and wild-type mice by quantitative PCR (AU, arbitrary units with respect to wild-type). **e** Serum leptin levels in $Cb2^{+/+}$ and $Cb2^{-/-}$ mice evaluated by ELISA. **f** Food intake was measured in non-treated $Cb2^{+/+}$ and $Cb2^{-/-}$ mice and in mice 1 day after leptin administration. Leptin was injected i.p. twice on a single day at a total dose of 1 μg/g. **g** Food intake. Results are percentages of baseline level and are mean ± SEM of 12 mice for each group. In **f** and **g**, +/+, $Cb2^{+/+}$; −/−, $Cb2^{-/-}$; *p<0.05 $Cb2^{-/-}$ vs wild-type in each treatment; †p<0.05 after vs before leptin injection (one-way ANOVA). **h** RT-PCR quantification of *Cnr1* mRNA in cerebellum (Cb), hypothalamus (HT) and eWAT of $Cb2^{+/+}$ and $Cb2^{-/-}$ mice. **i** RT-PCR quantification of *Srebf1c* and *Pck1* mRNA of $Cb2^{+/+}$ and $Cb2^{-/-}$ mice in eWAT. **j** Immunohistochemical analysis of white adipose tissue in 12-month-old $Cb2^{+/+}$ and $Cb2^{-/-}$ mice. Macrophages in adipose tissue of 12-month-old $Cb2^{+/+}$ and $Cb2^{-/-}$ mice were detected after immunohistochemical analysis using F4/80-specific antibody (×200). Arrow indicates infiltrated macrophage. **k** Chronic inflammatory responses in $Cb2^{+/+}$ and $Cb2^{-/-}$ mice. RT-PCR analysis revealed no differences in mRNA expression of *Tnfa*, *Ccl2* and *Il6* in eWAT tissue from $Cb2^{+/+}$ and $Cb2^{-/-}$ mice. Data are mean ± SEM of 12 mice for each group. +/+, $Cb2^{+/+}$; −/−, $Cb2^{-/-}$. *p<0.05 vs $Cb2^{+/+}$ (one-way ANOVA)

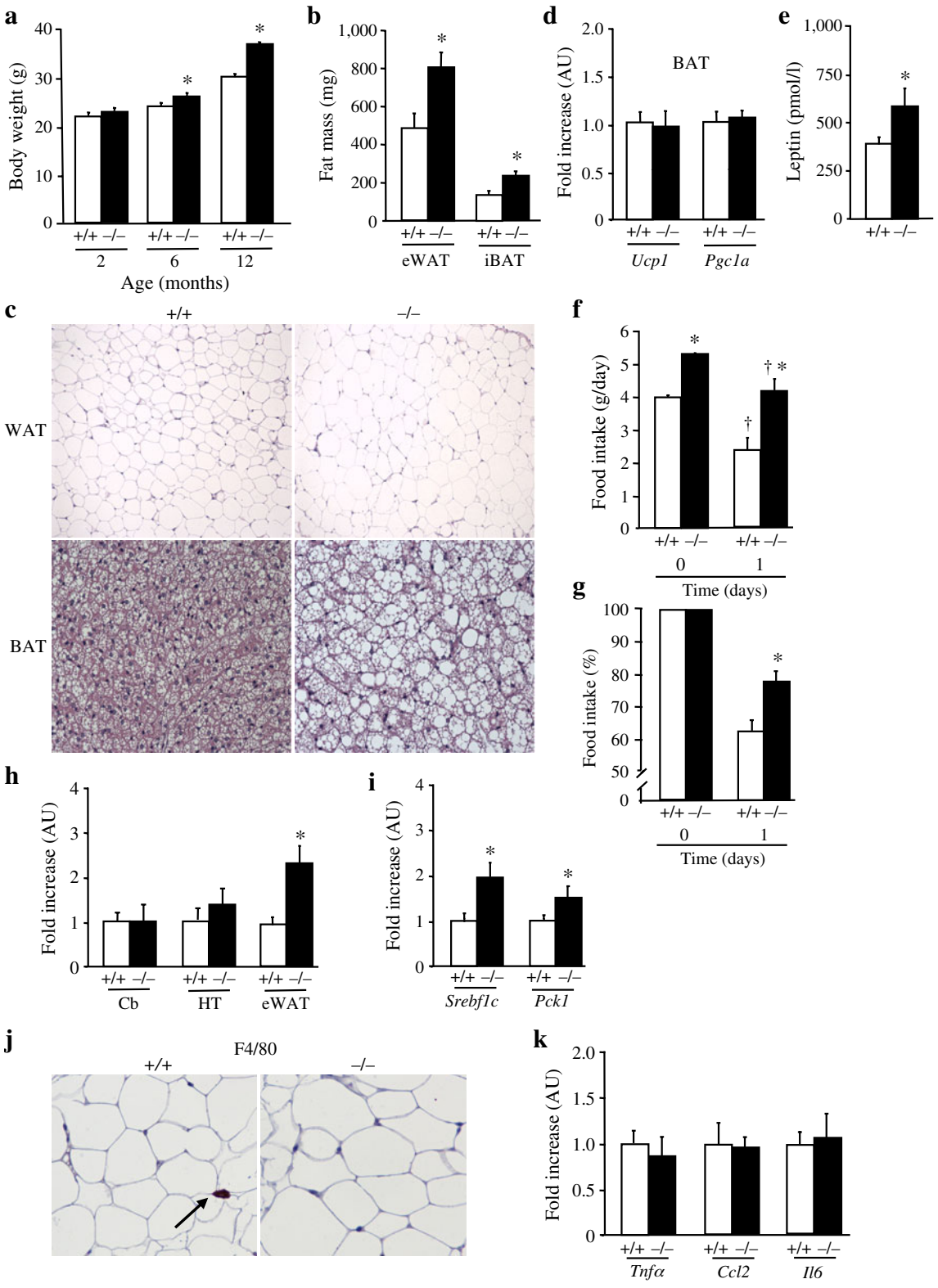

Cb2$^{-/-}$ mice showed higher mRNA levels of the transcription factor sterol regulatory element transcription factor 1c (*Srebf1c*) in epididymal WAT (Fig. 1i), a key positive regulator of lipogenesis [29], which can also be induced by CB1R [7]. Obesity is often associated with increased circulating Non-sterified fatty acid (NEFA) levels [30]. However, although 12-month-old *Cb2*$^{-/-}$ mice displayed increased body weight, they presented similar

NEFA levels to wild-type mice (0.5±0.06 vs 0.53± 0.05 mmol/l), suggesting that either lipolysis was not induced or that NEFA re-esterification was activated. Consistent with the latter, a 1.5-fold increase in expression in WAT of phosphoenolpyruvate carboxykinase (*Pck1*), a key regulatory enzyme of glyceroneogenesis, was observed in 12-month-old $Cb2^{-/-}$ mice (Fig. 1i).

Twelve-month-old obese $Cb2^{-/-}$ mice did not develop adipose tissue inflammation Obesity and type 2 diabetes are associated with chronic inflammation in WAT, characterised by increased production of cytokines, such as tumour necrosis factor-α (TNF-α), interleukin-6 (IL-6) and chemokine (C-C motif) ligand 2 (CCL2) [31]. In addition, CB2R, which is expressed in immune cells [32, 33], plays a major role in the modulation of obesity-associated inflammatory responses [24]. Despite adipose hypertrophy, no macrophage infiltration in WAT from obese 12-month-old $Cb2^{-/-}$ mice was observed after immunohistochemical analysis with F4/80 (Fig. 1j). In agreement, quantitative PCR analysis of WAT revealed similar expression levels of *Tnfa*, *Il6* and *Ccl2* in $Cb2^{-/-}$ obese mice compared with $Cb2^{+/+}$ mice (Fig. 1k). We also evaluated the inflammatory response of $Cb2^{-/-}$ mice after the acute administration of an external antigen. $Cb2^{+/+}$ and $Cb2^{-/-}$ mice were treated with an acute i.p. injection of LPS (0.5 mg/kg). Blood samples were obtained 3 and 12 h after treatment and TNF-α (3 h after injection) and IL-6 (12 h after injection) concentrations were measured by ELISA. However, no differences were observed between $Cb2^{+/+}$ and $Cb2^{-/-}$ mice (TNF-α: wild type, 646±101.85 vs $Cb2^{-/-}$, 1033±483.3 pg/ml; IL-6: wild type, 6048±1686 vs $Cb2^{-/-}$, 8822±1269 pg/ml), indicating that $Cb2^{-/-}$ mice were not protected from acute antigen-induced systemic inflammation.

Twelve-month-old $Cb2^{-/-}$ obese mice revealed enhanced insulin sensitivity and increased glucose uptake Twelve-month-old obese $Cb2^{-/-}$ mice were normoglycaemic (Fig. 2a) and reached a greater hypoglycaemic response during an insulin tolerance test (0.75 IU/kg i.p.; Fig. 2b). In addition, increased skeletal muscle glucose uptake was observed when FDG-PET analysis was performed (Fig. 2c–e). PET imaging revealed slightly lower FDG absorption in basal conditions in the anterior paws of $Cb2^{-/-}$ mice (Fig. 2c, d). However, $Cb2^{-/-}$ mice displayed higher forepaw FDG absorption than wild-type mice after an insulin administration, consistent with increased glucose uptake in response to the hormone (Fig. 2c, e). Nevertheless, this was not associated with further increased phosphorylation levels of either protein kinase B (AKT; Fig. 2f, g) or its substrate glycogen synthase-kinase 3B (GSK3B; Fig. 2h, i) in skeletal muscle. Moreover, when phosphorylation of insulin receptor (IR) and insulin receptor substrate 1 (IRS1) was determined, no differences were observed between wild-type and $Cb2^{-/-}$ mice (data not shown), indicating that the IR-AKT pathway was not further upregulated by insulin in $Cb2^{-/-}$ mice. In addition, wild-type and $Cb2^{-/-}$ mice showed similar GLUT4 protein levels (ESM Fig. 2f–h), indicating that enhanced skeletal muscle glucose uptake did not result from increased expression of this glucose transporter.

Therefore, in spite of weight gain with age, $Cb2^{-/-}$ mice showed improved insulin sensitivity, which agreed with the lack of adipose tissue inflammation and the normal circulating NEFA levels. The lack of CB2R in $Cb2^{-/-}$ mice also led to a 60% decrease in the expression of *Cnr1* in skeletal muscle (Fig. 2j), which could contribute to enhanced insulin sensitivity [34]. This decrease in *Cnr1* expression was also observed in 6-month-old non-obese $Cb2^{-/-}$ mice (ESM Fig. 2i).

CB2R antagonism resulted in improved insulin sensitivity To further investigate CB2R-mediated responses in vivo, 2-month-old mice were treated daily with i.p. injections of vehicle (control) or a selective CB_2 antagonist (SR 144528) for 4 weeks. After this period, antagonist-treated mice showed a slight, non-statistically significant increase in body weight gain compared with controls (Fig. 3a), but normal food intake (Fig. 3b) and hypothalamic expression of *Cnr1* (Fig. 3c). Moreover, these mice displayed no

Fig. 2 Enhanced insulin sensitivity and glucose uptake in skeletal muscle of $Cb2^{-/-}$ mice. **a** Blood glucose levels in fed condition in 12-month-old $Cb2^{+/+}$ and $Cb2^{-/-}$ mice. **b** Intraperitoneal insulin tolerance test. Insulin (0.75 IU/kg body weight) was injected intraperitoneally into fed $Cb2^{+/+}$ (white squares) and $Cb2^{-/-}$ (black squares) mice and blood samples were taken from the tail vein at the times indicated. Results are percentages of blood glucose value at time 0 and are mean ± SEM of 12 animals for each group. **c** PET images showing forepaw FDG absorption in basal conditions and after insulin (0.5 IU/kg) administration in $Cb2^{+/+}$ and $Cb2^{-/-}$ mice. **d** Forepaw FDG absorption (standardised uptake value, SUV) in basal condition after saline administration in $Cb2^{+/+}$ and $Cb2^{-/-}$ mice. *$p<0.05$ vs $Cb2^{+/+}$ (one-way ANOVA). **e** Insulin (0.5 IU/kg)-induced FDG absorption (SUV) in forepaws in $Cb2^{+/+}$ and $Cb2^{-/-}$ mice. Results are percentage increases in FDG absorption when compared with saline (n=4). +/+, $Cb2^{+/+}$; −/−, $Cb2^{-/-}$. *$p<0.05$ vs $Cb2^{+/+}$ (one-way ANOVA). **f**, **g** Western blot analysis of phosphorylated (P)Ser473-AKT and total AKT using tibialis muscle lysates from wild-type (WT; $Cb2^{+/+}$) and $Cb2^{-/-}$ mice: representative immunoblots (**f**) and densitometric analysis (**g**). Results are mean ± SEM and are percentage increases in P^{Ser473}-AKT after insulin injection when compared with the non-stimulated condition (n=3). White columns, wild type; black columns, $Cb2^{-/-}$. **h**, **i** Western blot analysis of phosphorylated (P)Ser9-GSK3B and total GSK3B using tibialis muscle lysates from wild-type (WT) and $Cb2^{-/-}$ mice: representative immunoblots (**h**) and densitometric analysis (**i**). Results are mean ± SEM and are expressed as percentage increases in P^{Ser9}-GSK3B after insulin injection when compared with the non-stimulated condition (n=3). White columns, wild type; black columns, $Cb2^{-/-}$. **j** Quantitative PCR analysis of *Cnr1* mRNA expression in skeletal muscle of $Cb2^{+/+}$ and $Cb2^{-/-}$ animals (n=4). Results are mean ± SEM. *$p<0.05$ vs $Cb2^{+/+}$

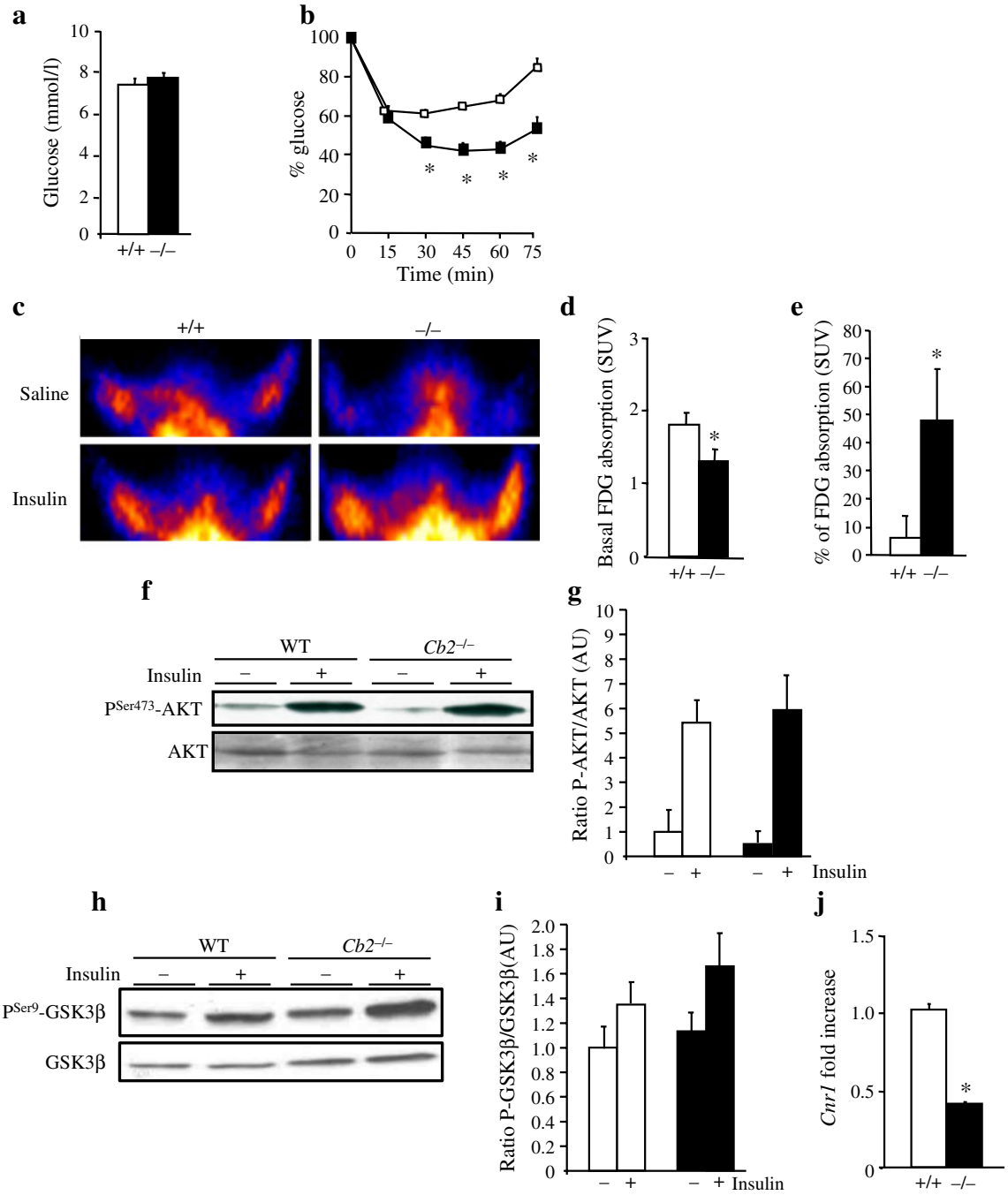

difference in epididymal WAT mass (430±25.3 vs 460±19.8 mg) and in *Cnr1* expression in WAT (Fig. 3c). Similarly, antagonist treatment of 3T3L1 adipocytes did not increase triacylglycerol content (ESM Fig. 3a, b), consistent with a lack of increased adipogenesis. In addition, antagonist-treated mice showed normal circulating levels of NEFA (0.43±0.04 vs 0.46±0.05 mmol/l) and triacylglycerol (71.3±5.6 vs 58.3±5.9 mg/dl) and normal glucose tolerance (Fig. 3d). After 4 weeks of treatment, antagonist-injected mice showed improved insulin sensitivity compared with vehicle-injected mice (Fig. 3f). No changes in *Cnr1* expression in skeletal muscle were observed (Fig. 3c), suggesting that decreased CB2R activation in skeletal muscle could be responsible for the increased insulin sensitivity in antagonist-treated wild-type mice.

$Cb2^{-/-}$ mice fed a high-fat diet showed reduced body weight gain and increased insulin sensitivity To examine whether the lack of CB2R could prevent diet-induced insulin resistance, 2-month-old $Cb2^{-/-}$ and $Cb2^{+/+}$ mice

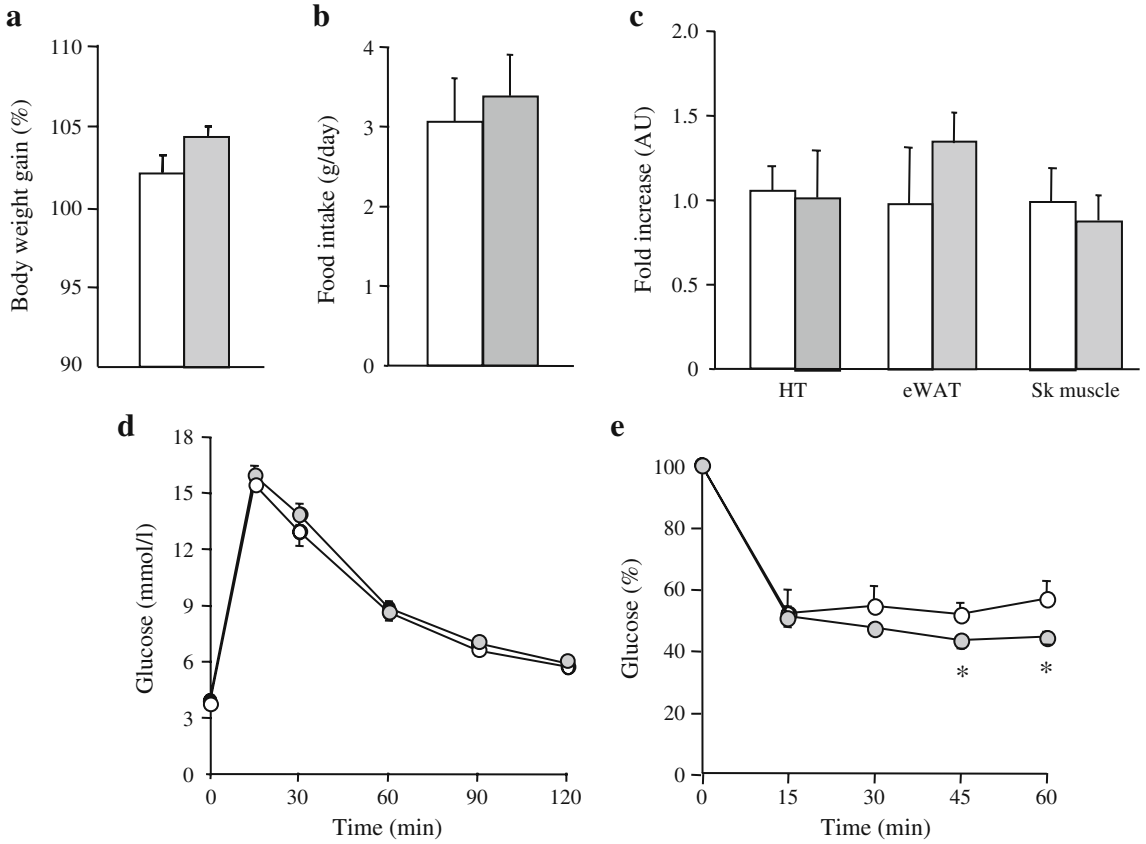

Fig. 3 Metabolic effects of CB2R antagonism in mice. **a** After 4 weeks of treatment with daily i.p. injections of vehicle (control; white columns) or the CB2 antagonist SR 144528 (grey columns), no difference was observed in body weight gain. **b** Food intake in antagonist-treated mice presented as g of food/day. **c** Antagonist treatment did not alter *Cnr1* expression in epididymal WAT (eWAT), hypothalamus (HT) or skeletal muscle (Sk muscle), as shown by RT-PCR analysis. **d** Intraperitoneal glucose tolerance test. Awake overnight-fasted control (white circles) and antagonist-treated (grey circles) mice were given an i.p. injection of glucose (1 g/kg). Blood samples were taken at the times indicated from the tail vein and glucose levels were measured. **e** Intraperitoneal insulin tolerance test. Insulin (0.75 IU/kg body weight) was injected intraperitoneally into fed antagonist-treated mice. Blood samples were taken at the times indicated from the tail vein of the same animal. Results are percentages of blood glucose values at time 0 for each mouse and are mean ± SEM for eight animals in each group. White circles, control mice; grey circles, antagonist-treated mice. *$p<0.05$ vs wild-type

were fed a high-fat diet for 8 weeks. Both groups developed obesity, but $Cb2^{-/-}$ mice on the high-fat diet showed reduced body weight gain (about 30% increase) compared with $Cb2^{+/+}$ mice on the high-fat diet (about 50% increase; Fig. 4a). Consistent with this, high fat fed $Cb2^{-/-}$ mice displayed decreased fat mass (Fig. 4b) and adipocyte mean area compared with high fat fed wild-type mice as measured by morphometric analysis of epididymal WAT sections (Fig. 4c). Although $Cb2^{-/-}$ mice fed a standard diet showed greater food intake than wild-type mice, no differences were observed between these groups of mice when fed a high-fat diet (Fig. 4d). Consistent with the similar food intake, *Cnr1* expression in the hypothalamus was not different between $Cb2^{+/+}$ and $Cb2^{-/-}$ mice on the high-fat diet (ESM Fig. 4a). Whole-body insulin sensitivity was also measured in an insulin tolerance test. High fat fed $Cb2^{-/-}$ mice displayed similar insulin sensitivity and similar insulinaemia compared with $Cb2^{+/+}$ mice fed a standard diet (Fig. 4e, f). Moreover, high fat fed $Cb2^{-/-}$ mice showed normal expression of *Cnr1* in skeletal muscle (ESM Fig. 4a). WAT from high fat fed $Cb2^{-/-}$ mice showed reduced macrophage infiltration and expression of the cytokine genes *Ccl2* and *Tnfa* compared with wild-type mice (Fig. 5a–d). In addition, serum levels of glucose, triacylglycerol, leptin and adiponectin remained similar in the two groups of mice (ESM Fig. 4b–e). Hepatic triacylglycerol storage was also markedly reduced in high fat fed $Cb2^{-/-}$ mice compared with high fat fed wild-type mice (Fig. 5e, f). Thus, the reduction in body weight gain in high fat fed $Cb2^{-/-}$ compared with $Cb2^{+/+}$ animals was parallel to improved adipose tissue inflammatory state, normal insulin sensitivity and hepatic lipid content. These results indicate that the lack of a CB2R-mediated response reduced body weight gain during the feeding of a hypercaloric diet and protected mice from diet-induced insulin resistance.

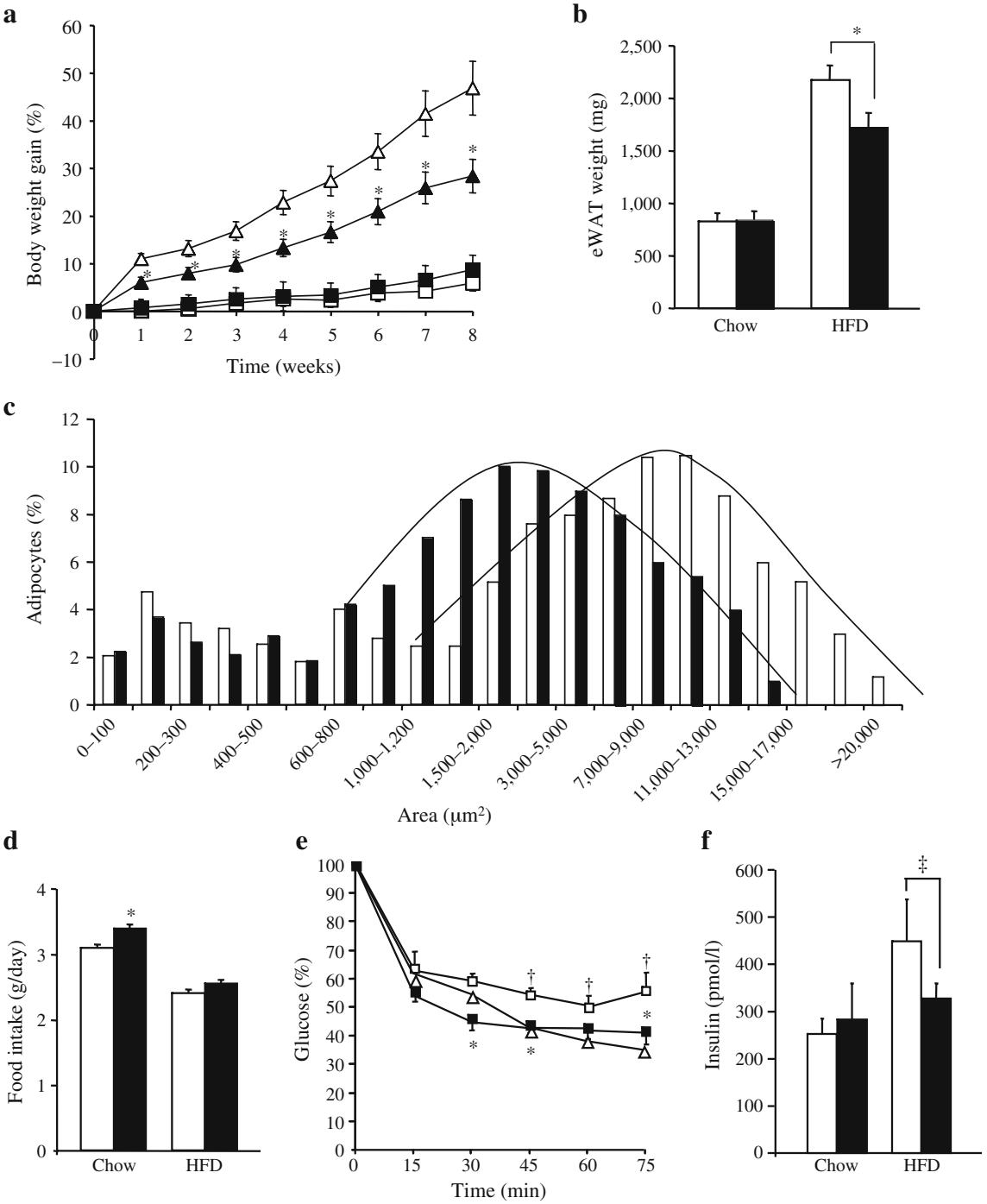

Fig. 4 *Cb2*$^{-/-}$ mice fed a high-fat diet showed decreased body weight gain and normal insulin sensitivity. Two-month-old male wild-type and *Cb2*$^{-/-}$ mice were fed a high-fat diet for 8 weeks. **a**, Body weight gain. White squares, wild type, standard diet; black squares, *Cb2*$^{-/-}$, standard diet; white triangles, wild type, high-fat diet; black triangles, *Cb2*$^{-/-}$, high-fat diet. (**b**) Epididymal fat pad weight (eWAT). In **b**–**d** and **f**, white columns, wild type; black columns, *Cb2*$^{-/-}$ (also applies to **c**, **d** and **f**) Chow, standard diet; HFD, high-fat diet. **c** Frequency distribution of adipocyte cell area from eWAT of wild-type and *Cb2*$^{-/-}$ mice fed a high-fat diet. Results are mean ± SEM of >3,500 adipocytes per group of mice. **d** Food intake in wild-type and *Cb2*$^{-/-}$ mice fed chow or a high-fat diet. **e** Insulin tolerance test. Insulin (0.75 IU/kg body weight) was injected i.p. into wild-type and *Cb2*$^{-/-}$ mice. Blood samples were taken from the tail vein at the times indicated and glucose levels were determined. White triangles, wild type, standard diet; white squares, wild type, high-fat diet; black squares, *Cb2*$^{-/-}$, high-fat diet. **f** Serum insulin was measured in fat-fed wild-type and *Cb2*$^{-/-}$ mice. Results are mean ± SEM of ten mice for each group. *$p<0.05$ *Cb2*$^{-/-}$ vs wild-type, †<0.05 chow fed vs high fat fed wild-type, ‡$p<0.05$ high-fat fed wild-type vs high fat fed *Cb2*$^{-/-}$

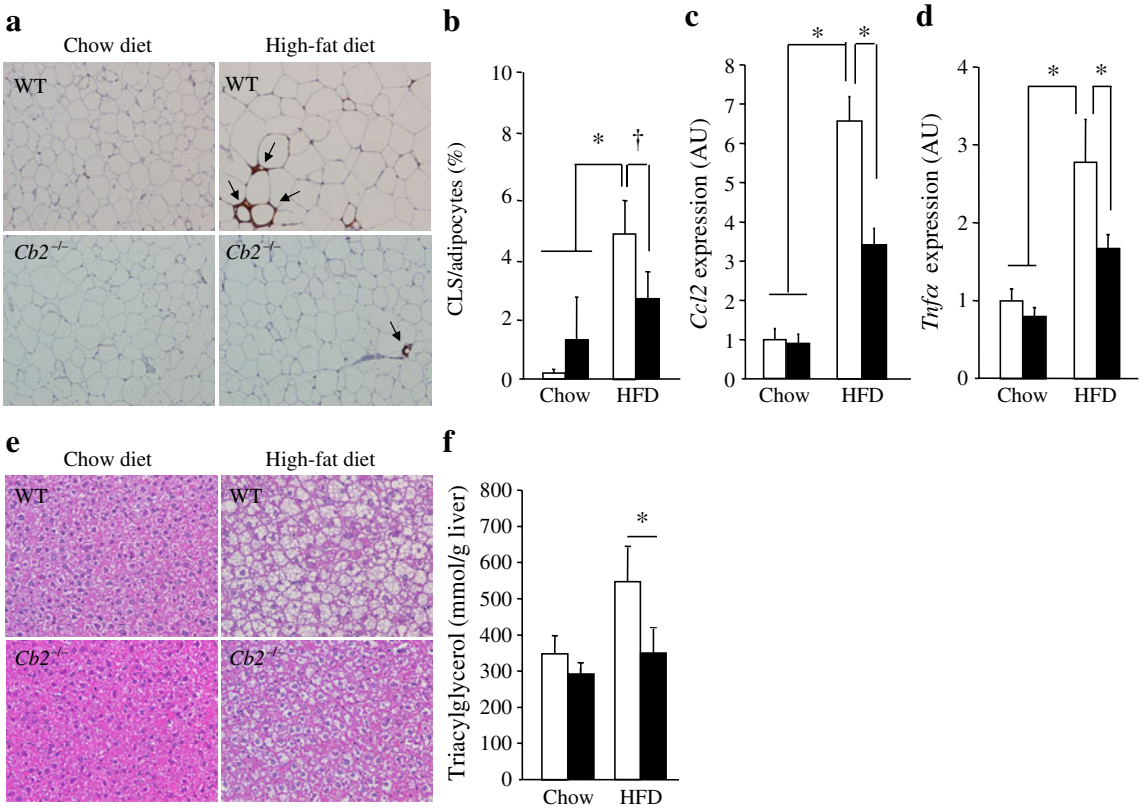

Fig. 5 Two-month-old *Cb2*$^{-/-}$ mice presented decreased adipose tissue inflammation compared with wild-type (WT) mice when both groups were fed a high-fat diet for 8 weeks. **a** Representative MAC-2 immunostaining of epididymal WAT sections from wild-type and *Cb2*$^{-/-}$ mice. MAC-2-stained cells (brown) surrounding adipocytes form crown-like structures (CLS). **b** The number of MAC-2-positive CLS per field was counted manually and the number of CLS per 1,000 adipocytes was used as a measure of adipose tissue macrophage content. Three mice per group were analysed. White columns, wild type; black columns, *Cb2*$^{-/-}$ (also applies to **c**, **d** and **f**). *$p<0.05$ vs wild-type mice on the high-fat diet; †$p<0.1$ HFD *Cb2*$^{-/-}$ vs HFD wild type. **c**, **d** Gene expression in adipose tissue from *Cb2*$^{-/-}$ mice was analysed by measuring relative mRNA levels using quantitative PCR for the proinflammatory cytokines *Ccl2* (**c**) and *Tnfa* (**d**). *$p<0.05$. **e**, **f** Hepatic steatosis was prevented in high fat fed *Cb2*$^{-/-}$ mice. **e** Representative sections stained with haematoxylin/eosin of liver from wild-type and *Cb2*$^{-/-}$ mice fed either a standard (chow) or a high-fat diet for 8 weeks. **f** Triacylglycerol content in the liver of wild-type and *Cb2*$^{-/-}$ mice. Data are mean ± SEM of eight mice for each group. *$p<0.05$

Discussion

Cb2$^{-/-}$ mice fed a standard diet displayed increased body weight gain and adipose tissue hypertrophy with age (older than 6 months), which was associated with increased food intake and hyperleptinaemia. In contrast, 2-month-old high fat fed *Cb2*$^{-/-}$ mice displayed reduced body weight gain and decreased fat pad mass compared with high fat fed wild-type mice. However, during high-fat feeding, no differences in food intake were observed, as described previously [24]. These results may suggest that while differences in food intake could explain long-term enhanced body weight during standard diet feeding, the lack of CB2R protected *Cb2*$^{-/-}$ mice from body weight gain during high fat feeding in young animals. Both CB1R and CB2R are present in white adipose tissue [35] and upregulation of CB1R activity in adipose tissue has been associated with increased lipogenesis and decreased lipolysis in obese humans and rodents [9, 10, 36]. Two- to 4-month-old *Cb2*$^{-/-}$ mice presented normal *Cnr1* expression in adipose tissue in both the standard and the high-fat feeding condition, suggesting that improved body weight in high fat fed animals was probably not due to decreased CB1R activity. However, adipose tissue of old *Cb2*$^{-/-}$ mice (older than 6 months) showed a gradual overexpression of *Cnr1* that increased in parallel to epididymal fat pad weight, suggesting that enhanced CB1R levels may be a consequence of the progressive adipose tissue hypertrophy. Treatment with a CB2R antagonist neither altered *Cnr1* expression in white adipose tissue nor increased fat pad mass, and these mice showed normal food intake. Moreover, the CB2R antagonist did not alter lipogenesis in isolated adipocytes, whereas the CB1R antagonist did [8]. This suggests that adipose tissue hypertrophy in *Cb2*$^{-/-}$ mice resulted from a long-term adaptive response to the constitutive lack of CB2R, which involved increased food intake. In

addition, although standard-fed *Cb2*$^{-/-}$ mice showed greater food intake, *Cnr1* expression was not increased in the hypothalamus, suggesting that lack of CB2R may directly induce signals that increase appetite. This phenotype was opposite to that of *cb1*$^{-/-}$ mice, which are leaner than *cb1*$^{+/+}$ mice and show reduced food intake [37].

In spite of the development of obesity, consistent with the results in high fat fed mice, insulin sensitivity was enhanced in 12-month-old *Cb2*$^{-/-}$ mice, as revealed by an improved insulin tolerance test. Moreover, PET imaging revealed an enhancement of skeletal muscle insulin-mediated glucose uptake in *Cb2*$^{-/-}$ mice. Similarly, CB1R antagonists facilitate skeletal muscle insulin-induced glucose uptake [38] and NEFA oxidation [34] and CB1R agonists can decrease insulin-induced responses in muscle cells [11]. Furthermore, a CB1R receptor inverse agonist increases glucose uptake both in muscle isolated from *ob*/*ob* mice and in cultured L6 muscle cells [38, 39]. The CB1R inhibition in muscle cells increases the signalling through the phosphatidyl inositol 3 (PI3) kinase pathway [38]. However, in skeletal muscle from insulin-treated *Cb2*$^{-/-}$ mice no further increase in either AKT or GSK3B phosphorylation levels were observed, suggesting that downstream signals may be involved in increasing insulin sensitivity. Thus, CB1R/CB2R activation may regulate the Ras/Raf/ERK cascade downstream of AKT while having little or no effect on components of the PI3 kinase/AKT pathway. Since skeletal muscle contains both CB1R and CB2R [22], improvement in insulin sensitivity could be related to the absence of CB2R and/or the downregulation of CB1R in skeletal muscle of *Cb2*$^{-/-}$ mice. Moreover, mice treated with CB2R antagonist showed increased insulin sensitivity with no changes in body weight or *Cnr1* expression. Thus, increased insulin sensitivity resulted from lack of CB2R in *Cb2*$^{-/-}$ mice rather than decreased *Cnr1* expression. Similarly, when fed a high-fat diet, *Cb2*$^{-/-}$ mice did not develop insulin resistance. This may have resulted from the fact that, although high fat fed *Cb2*$^{-/-}$ mice became obese, they showed lower body weight gain compared with high fat fed *Cb2*$^{+/+}$ mice. Indeed, high fat fed *Cb2*$^{-/-}$ mice gained about 30% in body weight, whereas *Cb2*$^{+/+}$ mice gained around 50%. High fat fed *Cb2*$^{-/-}$ mice displayed similar insulin sensitivity compared with standard-fed lean mice. Similarly, Deveaux et al. [24] have shown a reduction in body weight gain and improved insulin sensitivity in high-fat-fed *Cb2*$^{-/-}$ mice. In addition, high-fat-fed *Cb2*$^{-/-}$ mice showed reduced hepatic steatosis, which would also have contributed to improved insulin sensitivity. The absence of inflammatory responses in WAT could also be involved in the improvement of peripheral insulin sensitivity in *Cb2*$^{-/-}$ mice [24]. This agrees with the enhanced insulin sensitivity that was previously reported in obese mice with reduced WAT inflammation, such as *Tnf-α* (also known as *Tnf*)$^{-/-}$ [40], CCL2 or *Mcp-1*$^{-/-}$ [41] and osteopontin$^{-/-}$ mice [42]. The reduced adipose tissue macrophage infiltration and cytokine expression in high fat fed *Cb2*$^{-/-}$ mice was not associated with any alteration of *Cnr1* expression, suggesting that the lack of CB2R is responsible for the reduced inflammation. The increased glucose uptake described in *Cb2*$^{-/-}$ mice, together with the similar food intake compared with wild-type mice, may result in decreased body weight gain during high fat feeding.

In summary, this study reveals that genetic ablation of CB2R led to improved insulin sensitivity during both age-related and diet-induced insulin resistance. Thus, we demonstrated that CB2R plays an important role in glucose metabolism by modulating skeletal muscle insulin sensitivity and the inflammatory response in the adipose tissue. We provide new data confirming the key role of CB2R in the pathophysiology of obesity and type 2 diabetes, which may open new therapeutic approaches to counteract insulin resistance by using CB2R ligands.

Acknowledgements We thank S. Franckhauser and C. J. Mann for helpful discussions and L. Maggioni for technical support. This work was supported by grants from NIDA (5R01-DA016768 to R.M. and A. Zimmer), European Commission DG Research FP6 (GENADDICT #LSHM-CT-2004-05166 to R. Maldonado and A. Zimmer, PHECOMP #LSHM-CT-2007-037669 to R. Maldonado and EUGENE2, LSHM-CT-2004-512013 to F. Bosch), Ministerio de Ciencia e Innovación (SAF2007-64062 to R. Maldonado and SAF2005-01262 and SAF2008-00962 to F. Bosch), Instituto Salud Carlos III (RETICS-RTA #RD06/001/001 to R. Maldonado and CIBER de Diabetes y Enfermedades Metabólicas Asociadas to F. Bosch), the Deutsche Forschungsgemeinschaft (SFB645 to A. Zimmer) and Bundesministerium für Bildung und Forschung (NGFN2 to A. Zimmer).

Duality of interest R. Maldonado has received research grants from sanofi-aventis, Laboratorios Esteve and Ferrer. None of the other authors have relevant financial interests to disclose, nor a conflict of interest of any kind associated with this manuscript.

References

1. Pagotto U, Marsicano G, Cota D, Lutz B, Pasquali R (2006) The emerging role of the endocannabinoid system in endocrine regulation and energy balance. Endocr Rev 27:73–100
2. Scherer T, Buettner C (2009) The dysregulation of the endocannabinoid system in diabesity—a tricky problem. J Mol Med 87:663–668
3. Matsuda LA, Lolait SJ, Brownstein MJ, Young AC, Bonner TI (1990) Structure of a cannabinoid receptor and functional expression of the cloned cDNA. Nature 346:561–564
4. Munro S, Thomas KL, Abu-Shaar M (1993) Molecular characterization of a peripheral receptor for cannabinoids. Nature 365:61–65
5. Starowicz KM, Cristino L, Matias I et al (2008) Endocannabinoid dysregulation in the pancreas and adipose tissue of mice fed with a high-fat diet. Obesity (Silver Spring) 16:553–565

6. Di Marzo V, Goparaju SK, Wang L et al (2001) Leptin-regulated endocannabinoids are involved in maintaining food intake. Nature 410:822–825
7. Osei-Hyiaman D, DePetrillo M, Pacher P et al (2005) Endocannabinoid activation at hepatic CB1 receptors stimulates fatty acid synthesis and contributes to diet-induced obesity. J Clin Invest 115:1298–1305
8. Matias I, Gonthier MP, Orlando P et al (2006) Regulation, function, and dysregulation of endocannabinoids in models of adipose and beta-pancreatic cells and in obesity and hyperglycemia. J Clin Endocrinol Metab 91:3171–3180
9. Bluher M, Engeli S, Kloting N et al (2006) Dysregulation of the peripheral and adipose tissue endocannabinoid system in human abdominal obesity. Diabetes 55:3053–3060
10. Cote M, Matias I, Lemieux I et al (2007) Circulating endocannabinoid levels, abdominal adiposity and related cardiometabolic risk factors in obese men. Int J Obes (Lond) 31:692–699
11. Eckardt K, Sell H, Taube A et al (2009) Cannabinoid type 1 receptors in human skeletal muscle cells participate in the negative crosstalk between fat and muscle. Diabetologia 52:664–674
12. Lipina C, Stretton C, Hastings S et al (2010) Regulation of MAP kinase-directed mitogenic and protein kinase B-mediated signaling by cannabinoid receptor type 1 in skeletal muscle cells. Diabetes 59:375–385
13. Osei-Hyiaman D, Liu J, Zhou L et al (2008) Hepatic CB1 receptor is required for development of diet-induced steatosis, dyslipidemia, and insulin and leptin resistance in mice. J Clin Invest 118:3160–3169
14. Bensaid M, Gary-Bobo M, Esclangon A et al (2003) The cannabinoid CB1 receptor antagonist SR141716 increases Acrp30 mRNA expression in adipose tissue of obese fa/fa rats and in cultured adipocyte cells. Mol Pharmacol 63:908–914
15. Bermudez-Silva FJ, Sanchez-Vera I, Suarez J et al (2007) Role of cannabinoid CB2 receptors in glucose homeostasis in rats. Eur J Pharmacol 565:207–211
16. Howlett AC, Breivogel CS, Childers SR, Deadwyler SA, Hampson RE, Porrino LJ (2004) Cannabinoid physiology and pharmacology: 30 years of progress. Neuropharmacology 47 (Suppl 1):345–358
17. Galiegue S, Mary S, Marchand J et al (1995) Expression of central and peripheral cannabinoid receptors in human immune tissues and leukocyte subpopulations. Eur J Biochem 232:54–61
18. Mallat A, Lotersztajn S (2006) Endocannabinoids as novel mediators of liver diseases. J Endocrinol Invest 29:58–65
19. Murdolo G, Kempf K, Hammarstedt A, Herder C, Smith U, Jansson PA (2007) Insulin differentially modulates the peripheral endocannabinoid system in human subcutaneous abdominal adipose tissue from lean and obese individuals. J Endocrinol Invest 30:RC17–RC21
20. Spoto B, Fezza F, Parlongo G et al (2006) Human adipose tissue binds and metabolizes the endocannabinoids anandamide and 2-arachidonoylglycerol. Biochimie 88:1889–1897
21. Pagano C, Pilon C, Calcagno A et al (2007) The endogenous cannabinoid system stimulates glucose uptake in human fat cells via phosphatidylinositol 3-kinase and calcium-dependent mechanisms. J Clin Endocrinol Metab 92:4810–4819
22. Cavuoto P, McAinch AJ, Hatzinikolas G, Janovska A, Game P, Wittert GA (2007) The expression of receptors for endocannabinoids in human and rodent skeletal muscle. Biochem Biophys Res Commun 364:105–110
23. Juan-Pico P, Fuentes E, Bermudez-Silva FJ et al (2006) Cannabinoid receptors regulate Ca(2+) signals and insulin secretion in pancreatic beta-cell. Cell Calcium 39:155–162
24. Deveaux V, Cadoudal T, Ichigotani Y et al (2009) Cannabinoid CB2 receptor potentiates obesity-associated inflammation, insulin resistance and hepatic steatosis. PLoS One 4:e5844
25. Buckley NE, McCoy KL, Mezey E et al (2000) Immunomodulation by cannabinoids is absent in mice deficient for the cannabinoid CB(2) receptor. Eur J Pharmacol 396:141–149
26. Hamacher K, Coenen HH, Stocklin G (1986) Efficient stereospecific synthesis of no-carrier-added 2-[^{18}F]-fluoro-2-deoxy-D-glucose using aminopolyether supported nucleophilic substitution. J Nucl Med 27:235–238
27. Carr TP, Andresen CJ, Rudel LL (1993) Enzymatic determination of triglyceride, free cholesterol, and total cholesterol in tissue lipid extracts. Clin Biochem 26:39–42
28. Zhang F, Yang H, Wang Z et al (2007) Transient receptor potential vanilloid 1 activation induces inflammatory cytokine release in corneal epithelium through MAPK signaling. J Cell Physiol 213:730–739
29. Dulloo AG, Gubler M, Montani JP, Seydoux J, Solinas G (2004) Substrate cycling between de novo lipogenesis and lipid oxidation: a thermogenic mechanism against skeletal muscle lipotoxicity and glucolipotoxicity. Int J Obes Relat Metab Disord 28 (Suppl 4):S29–S37
30. Boden G (2001) Free fatty acids—the link between obesity and insulin resistance. Endocr Pract 7:44–51
31. Alexandraki K, Piperi C, Kalofoutis C, Singh J, Alaveras A, Kalofoutis A (2006) Inflammatory process in type 2 diabetes: the role of cytokines. Ann N Y Acad Sci 1084:89–117
32. Klein TW, Newton C, Larsen K et al (2003) The cannabinoid system and immune modulation. J Leukoc Biol 74:486–496
33. Karsak M, Gaffal E, Date R et al (2007) Attenuation of allergic contact dermatitis through the endocannabinoid system. Science 316:1494–1497
34. Cavuoto P, McAinch AJ, Hatzinikolas G, Cameron-Smith D, Wittert GA (2007) Effects of cannabinoid receptors on skeletal muscle oxidative pathways. Mol Cell Endocrinol 267:63–69
35. Roche R, Hoareau L, Bes-Houtmann S et al (2006) Presence of the cannabinoid receptors, CB1 and CB2, in human omental and subcutaneous adipocytes. Histochem Cell Biol 126:177–187
36. Jbilo O, Ravinet-Trillou C, Arnone M et al (2005) The CB1 receptor antagonist rimonabant reverses the diet-induced obesity phenotype through the regulation of lipolysis and energy balance. FASEB J 19:1567–1569
37. Cota D, Marsicano G, Tschop M et al (2003) The endogenous cannabinoid system affects energy balance via central orexigenic drive and peripheral lipogenesis. J Clin Invest 112:423–431
38. Liu YL, Connoley IP, Wilson CA, Stock MJ (2005) Effects of the cannabinoid CB1 receptor antagonist SR141716 on oxygen consumption and soleus muscle glucose uptake in Lep(ob)/Lep (ob) mice. Int J Obes (Lond) 29:183–187
39. Esposito I, Proto MC, Gazzerro P et al (2008) The cannabinoid CB1 receptor antagonist rimonabant stimulates 2-deoxyglucose uptake in skeletal muscle cells by regulating the expression of phosphatidylinositol-3-kinase. Mol Pharmacol 74:1678–1686
40. Uysal KT, Wiesbrock SM, Marino MW, Hotamisligil GS (1997) Protection from obesity-induced insulin resistance in mice lacking TNF-alpha function. Nature 389:610–614
41. Kanda H, Tateya S, Tamori Y et al (2006) MCP-1 contributes to macrophage infiltration into adipose tissue, insulin resistance, and hepatic steatosis in obesity. J Clin Invest 116:1494–1505
42. Nomiyama T, Perez-Tilve D, Ogawa D et al (2007) Osteopontin mediates obesity-induced adipose tissue macrophage infiltration and insulin resistance in mice. J Clin Invest 117:2877–2888